Supporting information

C-F-rich oil drop as non-expendable fluid interface modifier with low surface energy to stabilize Li metal anode

Qifan Yang [a,b,c], Jiulin Hu [a,c], Junwei Meng [a,b,c], Chilin Li [a,b,c,*]

[a] State Key Laboratory of High Performance Ceramics and Superfine Microstructure, Shanghai Institute of Ceramics, Chinese Academy of Sciences, 585 He Shuo Road, Shanghai 201899, China. Email: chilinli@mail.sic.ac.cn

[b] Center of Materials Science and Optoelectronics Engineering, University of Chinese Academy of Sciences, Beijing 100049, China.

[c] CAS Key Laboratory of Materials for Energy Conversion, Shanghai Institute of Ceramics, Chinese Academy of Sciences, Shanghai 201899, China

Experimental Section

Material Preparation. Perfluoropolyether (PFPE), i.e. polyperfluoromethyl isopropyl ether $CF_3O[-CF(CF_3)CF_2O-]_x(-CF_2O-)_yCF_3$, purchased from Aladdin corp.) was used. A drop of PFPE was transferred onto the surface of polished Li metal by a pipette under Ar atmosphere in the glove box. After the surface is well wetted and covered by PFPE, the modified anode was prepared for the following cell assembling.

Electrochemical Measurement. Electrochemical experiments were carried out by using coin cells in a LAND-CT2001A battery system. CR2032 type coin cells of two-electrode configuration were used to perform the galvanostatic measurement. Symmetric Li/Li and asymmetric Cu/Li cells were assembled to test the Li plating and stripping performance at different current densities. Li/Li cells were tested in the carbonate-based electrolyte with 1M $LiPF_6$ in ethylene carbonate (EC) and dimethyl carbonate (DMC) (1:1 in volume). Cu/Li cells were characterized in the ether-based electrolyte with 1M bistrifluoromethanesulfonimide lithium salt (LiTFSI) and 0.2M

$LiNO_3$ additive in dimethyl ether (DME) and 1,3-dioxolane (DOL) (1:1 in volume), as well as in the above-mentioned carbonate system. $LiNi_{0.8}Mn_{0.1}Co_{0.1}O_2$ (NMC811)/Li, $LiFePO_4$/Li and $LiNi_{0.8}Co_{0.15}Al_{0.05}O_2$(NCA)/Li full cells based on the carbonate-based electrolyte were cycled in a voltage range of 3-4.5 V, 3-4.3 V and 2.0-3.8 V at different rates respectively. Glass fiber (GF/B, Whatman) was applied as a separator. The electrolyte amount is 120 μL. The electrochemical impedance spectra (EIS) were done by using a Solartron frequency analyzer (1260−1296) in a frequency range of 10^{-2}−10^{6} Hz. The Cu/Li cells used for EIS measurement was priorly cycled at 1 mA cm^{-2} with a capacity of 2 mAh cm^{-2} in ether electrolyte. The exchange current density (I_0) was estimated based on the linear sweep voltammetry (LSV, VersaSTAT3, AMETEK Scientific Instruments) for Li/Li cells at a scanning rate of 0.1 mV s^{-1} in a voltage window of −0.2–0.2 V. The cation transference number (t_+) was estimated based on Potentiostatic Polarization method by comparing the EIS of Li/Li cells before and after polaization via Solartron frequency analyzer (1260−1296). The direct current polarization measurement in this method was performed on an electrochemical workstation (VersaSTAT3, AMETEK Scientific Instruments) with a voltage bias of 5 mV to obtain the initial and steady-state currents.

Material Characterization. For the scanning electron microscopy (SEM) observation of cycled electrode surface morphology, the cycled Li/Li and Cu/Li cells cycled at plating state were disassembled in an argon-filled glovebox. The cycled electrodes were washed by DMC or DME to remove the residual electrolyte salt. After dried, they were sealed in an argon-filled container and then quickly transferred into the SEM equipment (Magellan 400L, FEI) for observation. X-ray photoelectron spectroscopy (XPS, ESCAlab-250) analysis was performed to characterize the surface components of the pristine and cycled Li electrodes. The cycled Li electrodes were disassembled from the Li/Li cells after 5 cycles at plating state in carbonate electrolyte. The contact angle test for oil drop on Cu surface was carried on contact angle measuring instrument SDC200.

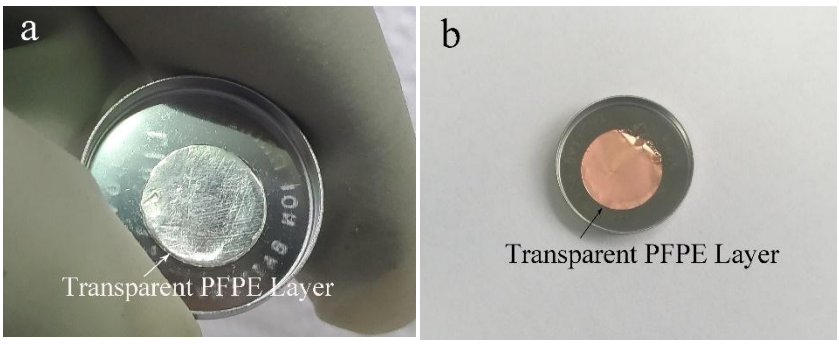

Figure S1. Digital photos of transparent PFPE oil layer spread on (a) Li anode surface and (b) Cu electrode surface.

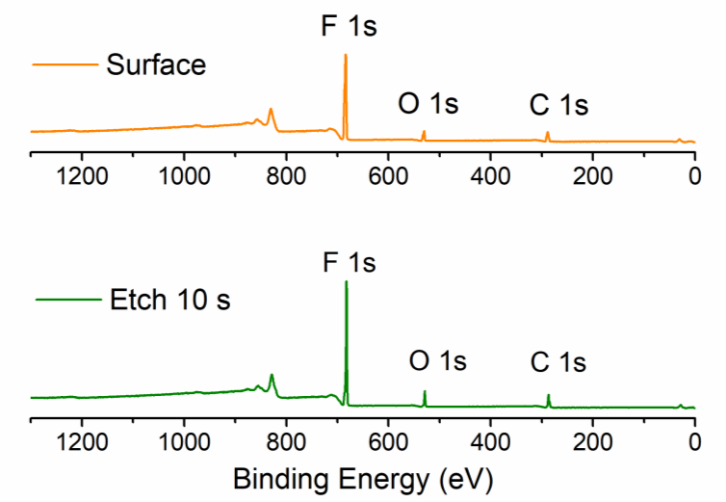

Figure S2. Survey XPS spectra of PFPE modified Li surface at pristine state in full binding energy range.

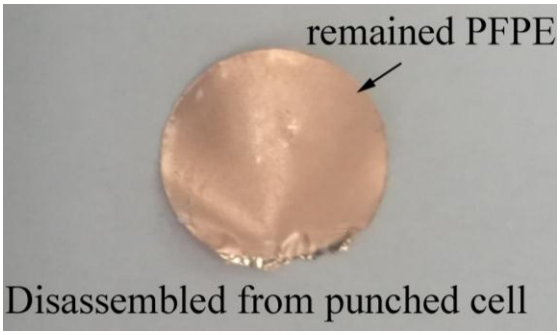

Figure S3. Digital photo of residual PFPE oil on Cu electrode from disassembled coin type cell.

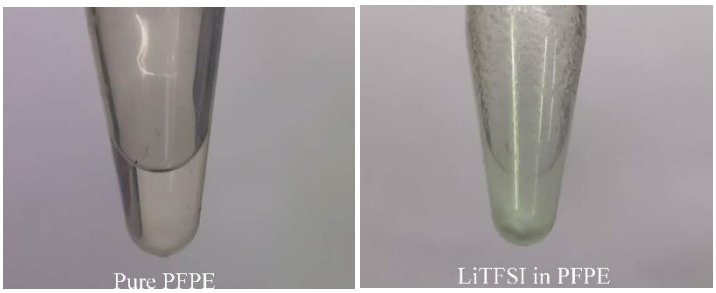

Figure S4. Digital photos of Li salt solubility test in PFPE (LiTFSI: 0.1mg, PFPE: 120 μL).

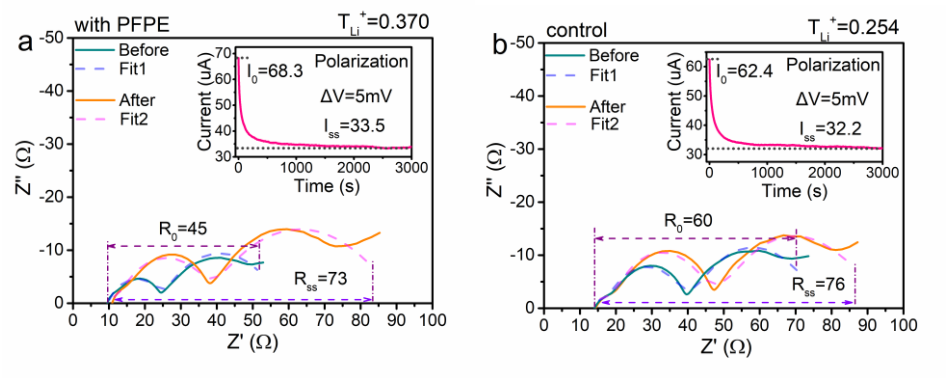

Figure S5. EIS of Li/Li cells before and after polarization for the estimation of Li^+ transferrence number: (a) under the effect of PFPE modification and (b) the control case at plated state after 40 cycles at 1 mA cm^{-2} (2 mAh cm^{-2}) in $LiPF_6$–EC–DMC systems. Insets: correnponding direct current polarization curves.

For this Potentiostatic Polarization method, under a small potential polarization (≤10 mV), the transference number for cation (t_+) is given by

$$t_+ = \frac{I_{SS}(\Delta V - I_0 R_0)}{I_0(\Delta V - I_{SS} R_{SS})} \quad (1)$$

where I_0 is the initial current, I_{ss} is the steady-state current, ΔV is the applied voltage bias, R_0 and R_{ss} are the interface resistances of cells before and after the polarization, respectively.

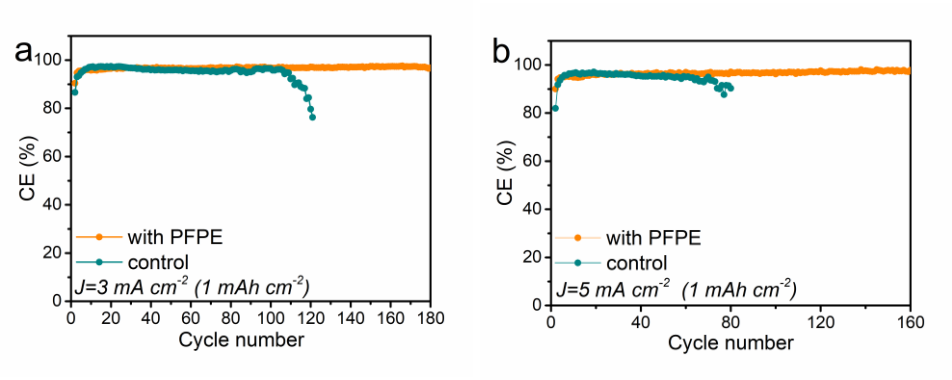

Figure S6. Cycling performance and CE evolution of Cu/Li asymmetric cells with and without PFPE modification at the current densities of (a) 3 mA cm^{-2} (1 mAh cm^{-2}) and (b) 5 mA cm^{-2} (1 mAh cm^{-2}).

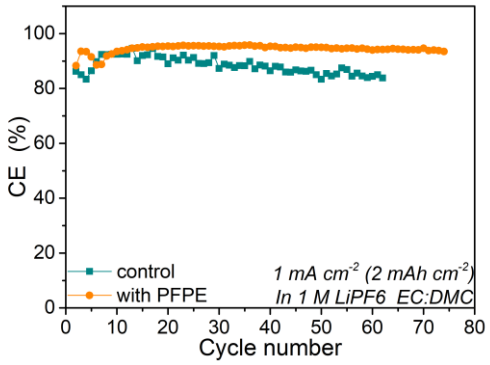

Figure S7. Cycling performance and CE evolution of Cu/Li asymmetric cells with and without PFPE modification at the current density of 1 mA cm^{-2} (2 mAh cm^{-2}) in carbonate electrolyte system.

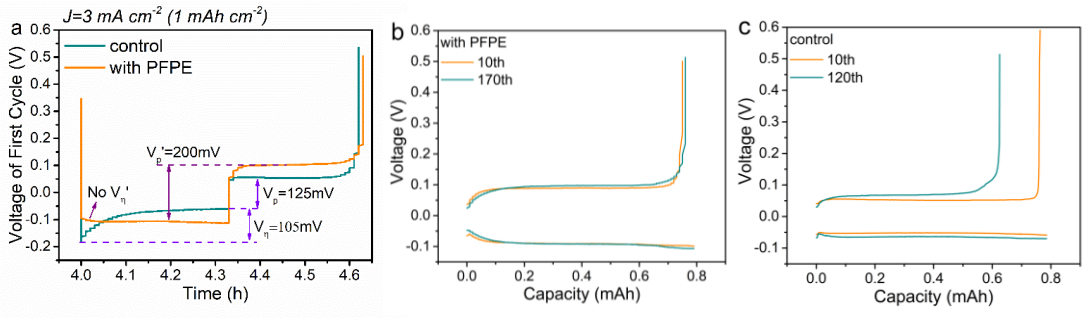

Figure S8. (a) Voltage-time profiles of Cu/Li cells with and without PFPE modification during the first cycle at 3 mA cm^{-2}. (b) Corresponding voltage-capacity

profiles for the cases (b) with and (c) without PFPE. V_η' and V_η are the nuclei overpotentials for the cases with and without PFPE respectively. V_p' and V_p are the plateau overpotentials for the cases with and without PFPE respectively.

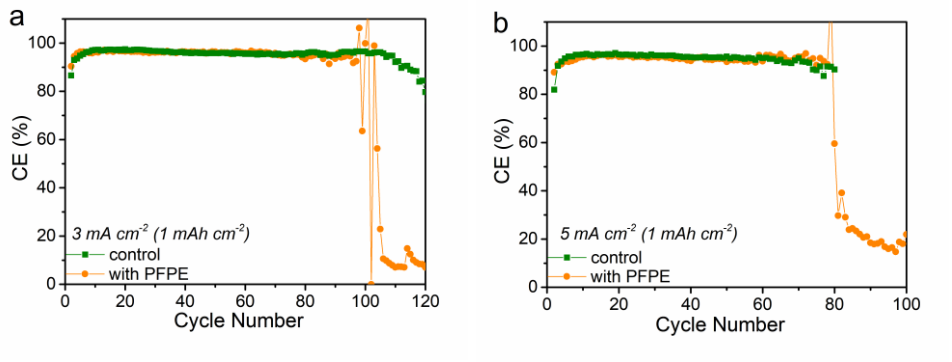

Figure S9. Cycling performance and CE evolution of Cu/Li asymmetric cells after increasing the drop amount of PFPE to four drops at the current densities of (a) 3 mA cm^{-2} and (b) 5 mA cm^{-2} with a capacity of 1 mAh cm^{-2}.

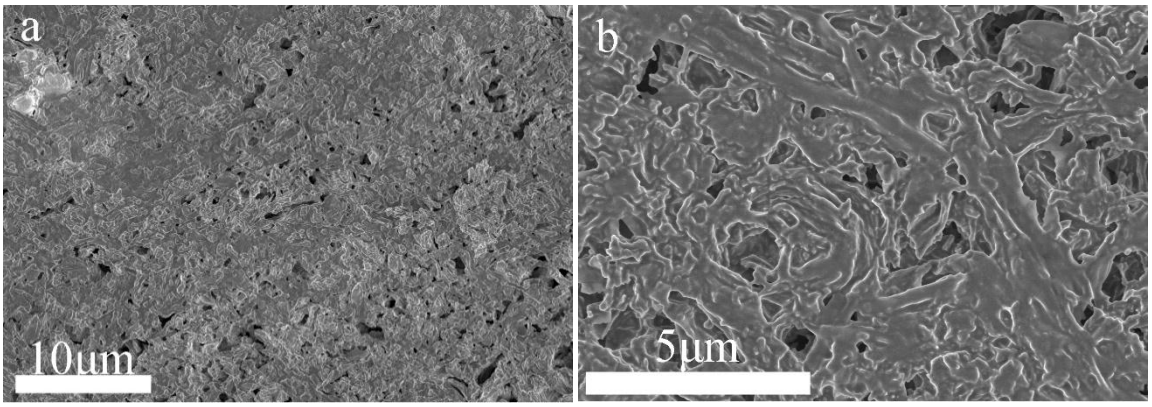

Figure S10. (a) Overview and (b) mognified SEM images of deposited Li on PFPE coated Cu electrode after 40 cycles.

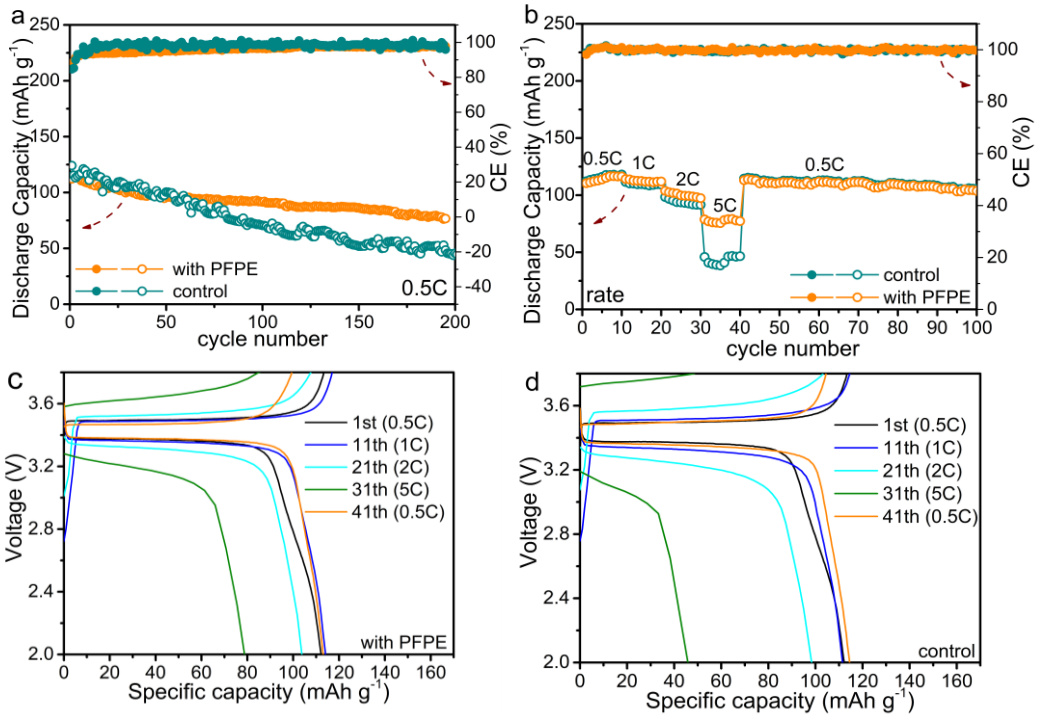

Figure S11. (a) Cycling performance of $LiFePO_4$/Li cells with and without PFPE modification at 0.5 C. (b) Rate performance of $LiFePO_4$/Li cells with and without PFPE modification. Corresponding voltage-capacity profiles of (c) modified and (d) control full cells at different rates.

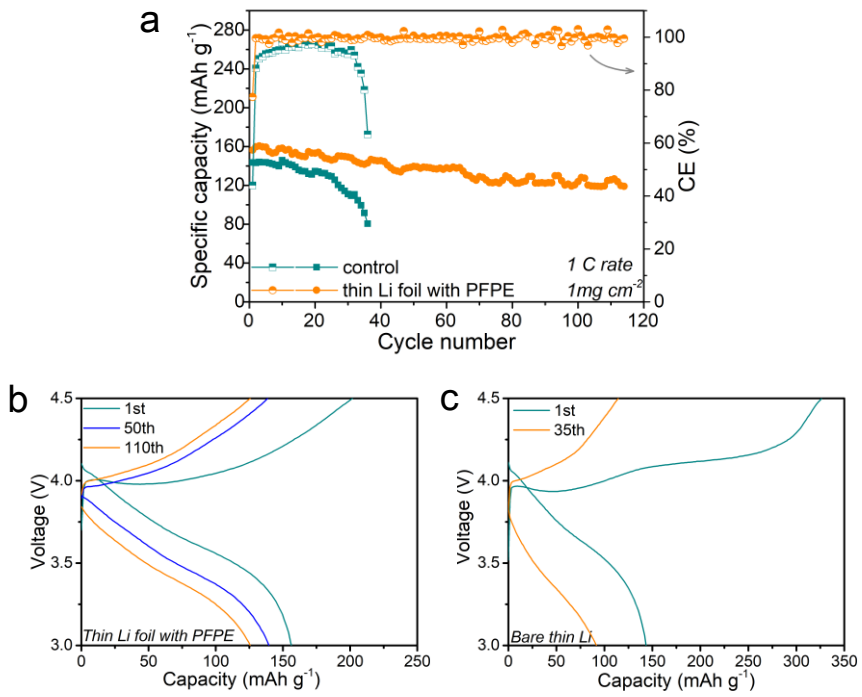

Figure S12. (a) Cycling performance of NCM811/thin Li full cells with and without PFPE modification at 1 C. Corresponding voltage-capacity profiles of (b) modified and (c) control full cells at different cycling stages.

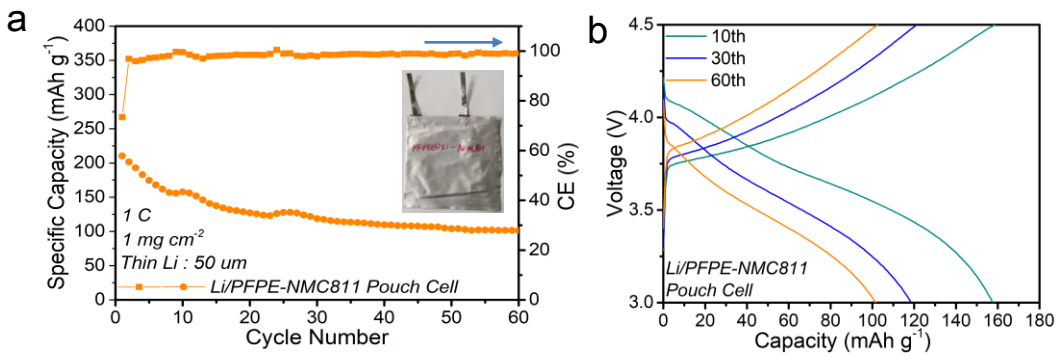

Figure S13. (a) Cycling performance of NCM811/thin Li pouch cell with PFPE modification at 1 C. (b) Corresponding voltage-capacity profiles of pouch full cell at different cycling stages.

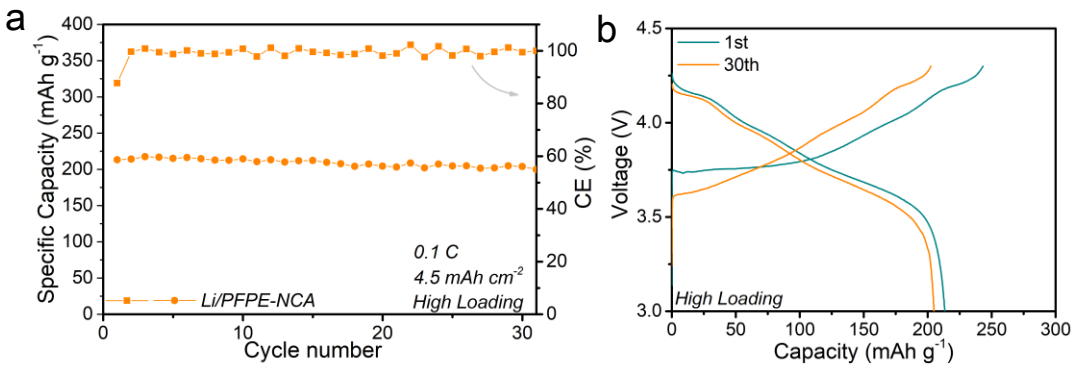

Figure S14. (a) Cycling performance of PFPE modified NCA/Li full cell with an area capacity of cathode as high as 4.5 mAh cm^{-2} at 0.1 C. (b) Corresponding voltage-capacity profiles of high-loading full cell at different cycling stages.